

## Critical optical coupling between a GaAs disk and a nanowaveguide suspended on the chip

C. Baker, C. Belacel, A. Andronico, P. Senellart, A. Lemaitre et al.

Citation: *Appl. Phys. Lett.* **99**, 151117 (2011); doi: 10.1063/1.3651493

View online: <http://dx.doi.org/10.1063/1.3651493>

View Table of Contents: <http://apl.aip.org/resource/1/APPLAB/v99/i15>

Published by the [American Institute of Physics](#).

---

### Related Articles

Low-loss polymer waveguides on nanoporous layers  
*Appl. Phys. Lett.* **99**, 153301 (2011)

Low-loss polymer waveguides on nanoporous layers  
*APL: Org. Electron. Photonics* **4**, 216 (2011)

Room temperature direct gap electroluminescence from Ge/Si0.15Ge0.85 multiple quantum well waveguide  
*Appl. Phys. Lett.* **99**, 141106 (2011)

Wideband ultraflat slow light with large group index in a W1 photonic crystal waveguide  
*J. Appl. Phys.* **110**, 063103 (2011)

Inverse polarizing effect of subwavelength metallic gratings in deep ultraviolet band  
*Appl. Phys. Lett.* **99**, 071103 (2011)

---

### Additional information on *Appl. Phys. Lett.*

Journal Homepage: <http://apl.aip.org/>

Journal Information: [http://apl.aip.org/about/about\\_the\\_journal](http://apl.aip.org/about/about_the_journal)

Top downloads: [http://apl.aip.org/features/most\\_downloaded](http://apl.aip.org/features/most_downloaded)

Information for Authors: <http://apl.aip.org/authors>

---

### ADVERTISEMENT



**AIP Advances**

**Submit Now**

Explore AIP's new  
open-access journal

- Article-level metrics now available
- Join the conversation! Rate & comment on articles

# Critical optical coupling between a GaAs disk and a nanowaveguide suspended on the chip

C. Baker,<sup>1</sup> C. Belacel,<sup>2</sup> A. Andronico,<sup>1</sup> P. Senellart,<sup>2</sup> A. Lemaitre,<sup>2</sup> E. Galopin,<sup>2</sup> S. Ducci,<sup>1</sup> G. Leo,<sup>1</sup> and I. Favero<sup>1,a)</sup>

<sup>1</sup>Laboratoire Matériaux et Phénomènes Quantiques, Université Paris Diderot, Sorbonne Paris Cité, CNRS-UMR 7162, 10 rue Alice Domon et Léonie Duquet, 75013 Paris, France

<sup>2</sup>Laboratoire de Photonique et Nanostructures, CNRS, Route de Nozay, 91460 Marcoussis, France

(Received 2 August 2011; accepted 21 September 2011; published online 14 October 2011)

We report on an integrated GaAs disk/waveguide system. A millimeter-long waveguide is suspended and tapered on the chip over a length of  $25\text{ }\mu\text{m}$  to evanescently couple to high Q optical whispering gallery modes of a GaAs disk. The critical coupling regime is obtained both by varying the disk/guide gap distance and the width of the suspended nanoscale taper. Experimental results are in good agreement with predictions from coupled mode theory. © 2011 American Institute of Physics. [doi:10.1063/1.3651493]

Whispering gallery mode (WGM) gallium arsenide (GaAs) optical cavities combine the optical properties of GaAs with small mode volumes and high quality factors Q, enabling a boost of light-matter interaction in different contexts: in quantum electrodynamics experiments,<sup>1–3</sup> for the realization of lasers,<sup>4</sup> in non-linear optics,<sup>5</sup> and now in optomechanics experiments.<sup>6–8</sup> The best Q factors on GaAs WGM cavities are of a few  $10^5$ , measured by evanescent coupling to an optical fiber taper.<sup>6,8,9</sup> However, fiber tapers suffer from a poor mechanical stability and are affected by a rapid degradation in standard humidity.<sup>10</sup> An integrated optics approach, with direct access to the cavity by an on-chip bus waveguide, can increase the range of operation of GaAs WGM cavities.<sup>11</sup> For example, a GaAs waveguide/disk structure was developed<sup>12</sup> and optically probed through a narrow-band grating coupler, allowing observing evanescent coupling in the under-coupled regime. However, for many applications, obtaining the critical coupling is crucial.<sup>13</sup> This applies in optomechanics<sup>14–16</sup> where maximal number of photons in the cavity is for example needed to reach optomechanical self-oscillation.<sup>17–19</sup>

Here, we investigate a GaAs waveguide/disk integrated structure but adopt direct injection at the cleaved facet of the guide, with a two-fold advantage: first, simple optics is used for waveguide coupling; second, the coupling is wavelength independent, allowing broadband (100 nm) spectroscopy of the system. We observe evanescent coupling and by varying the disk/guide gap distance or the guide taper width, the overlap between the disk and guide optical modes is adjusted and the important critical coupling regime is reached in a controlled manner. Our experimental results are in good agreement with coupled mode theory (CMT) expectations.<sup>20,21</sup>

We employ a semi-insulating GaAs substrate, on which we grow epitaxially a GaAs 500 nm buffer layer, a  $1.8\text{ }\mu\text{m}$   $\text{Al}_{0.8}\text{Ga}_{0.2}\text{As}$  sacrificial layer, and finally a 200 nm GaAs top layer. The guides and disks are defined by e-beam lithography with a negative resist. We draw straight optical waveguides 5  $\mu\text{m}$  wide and 2 mm long, extending up to the sample facets (Fig. 1(a)). The central region of each guide is

tapered in the vicinity of the target disk, to allow evanescent coupling (Inset of Fig. 1(a)). The nominal disk diameter is  $7.4\text{ }\mu\text{m}$ . In a first non-selective wet-etch, we separate the guide from the disk and define the boundaries of the guiding structures, etching away the 200 nm of GaAs. In a second etch step, we use hydrofluoric acid to under-etch the AlGaAs layer. First, this results in locally suspending both the disk and the waveguide (see Fig. 1(b)) with a sub-micron gap between the two (see Fig. 1(c)). Second, the lateral edges of the 5- $\mu\text{m}$  wide waveguide are under-etched on their whole length, resulting in a rail-like guiding structure (Fig. 1(d)). In this structure the transverse electric (TE), in-plane polarized, fundamental mode is confined in the 200 nm GaAs layer by semiconductor/air interfaces, with a small residual leaking into the substrate, which reduces the guide transmission when increasing the wavelength. Conversely, beam propagation method (BPM) simulations predict that the out-of-plane polarized (TM) fundamental mode leaks importantly into the substrate, leading to important optical losses of the rail-guide, which are confirmed experimentally. As a result, our waveguides efficiently select TE polarization. For the taper profile, we have chosen a 3-part linear profile, with lengths of 10, 5, and  $10\text{ }\mu\text{m}$ . The width of the central taper part is chosen to generally ensure a single TE guided mode. For these profiles, BPM calculations predict a transmission of the TE fundamental mode through the taper over 90%.

Optical spectroscopy of the disk/waveguide is performed in the 1300–1400 nm band using a CW external cavity diode laser, whose beam is focused onto the guide input facet using a micro-lensed fiber. The TE polarization is selected. Output light is collected by a microscope objective and sent on a p-i-n-photodetector. Fig. 2 shows the normalized transmission of a guide evanescently coupled to a disk as a function of the laser wavelength. Several resonances appear in this spectrum: they correspond to WGMs of the disk, whose loaded Q factors can reach 55 000, as shown in the inset of Fig. 2. This corresponds to intrinsic optical Q in the high  $10^4$  range. We note pronounced Fano profiles involving broad and fine optical resonances. Similar profiles, observed on Silica WGM toroid cavities coupled to a fiber taper, were attributed to interference between different modes of the cavity.<sup>22</sup>

<sup>a)</sup>Electronic mail: ivan.favero@univ-paris-diderot.fr.

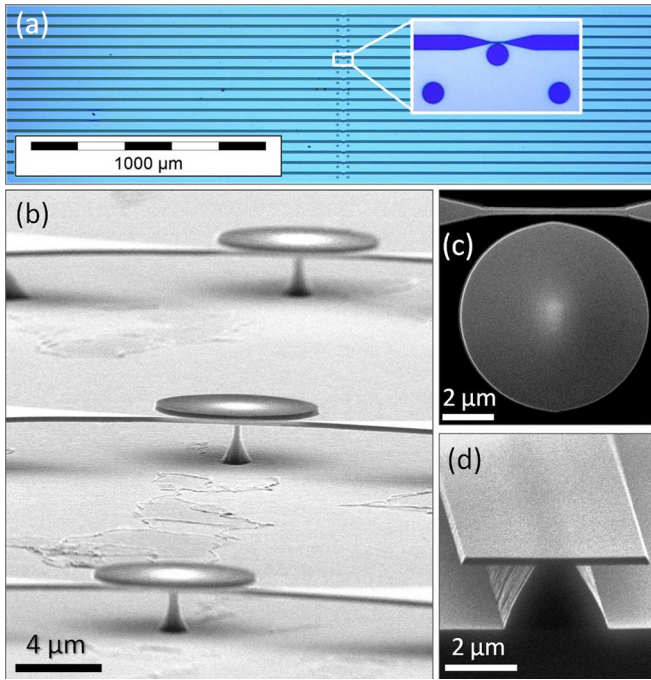


FIG. 1. (Color online) (a) Optical top view of the complete sample, containing 16 guide/disk lines. Inset: tapered part of the guide in the disk vicinity. The two other disks are fabrication witnesses. (b) SEM side-view of 3 disk/waveguide systems. (c) SEM top view of the central part of the tapered waveguide next to a disk. (d) SEM side view of the cleaved facet of the rail-guide.

Here, we focus on the fine control of the disk/waveguide evanescent coupling, in order to reach critical coupling where intrinsic and coupling losses of the cavity are equal. Our first strategy is to vary the gap distance  $g$  between disk and guide.<sup>8,13,23</sup> Fig. 3(a) shows transmission spectra obtained by varying  $g$ , keeping a constant taper width of 320 nm. From spectra 1–8,  $g$  is reduced in 25 nm steps from 350 to 190 nm. The gap distances are measured in a scanning electron microscope (SEM) with an uncertainty of  $\pm 7$  nm and agree within 5% with nominal values. In spectra 5–8 most notably, several resonances approach zero transmission, reflecting critical coupling.

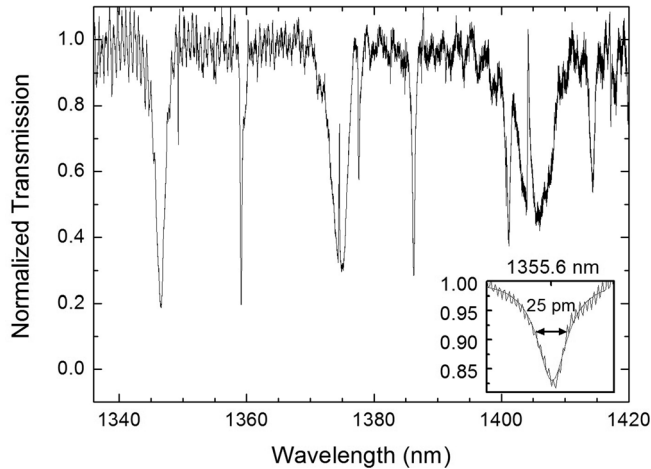


FIG. 2. Transmission spectrum of a suspended tapered waveguide coupled to a  $7.4 \mu\text{m}$  diameter GaAs disk. Inset: a fine optical resonance at  $\lambda = 1355 \text{ nm}$ , measured on another disk. The small amplitude oscillations in the base transmission correspond to Fabry-Perot fringes of the waveguide and are not noisy in nature.

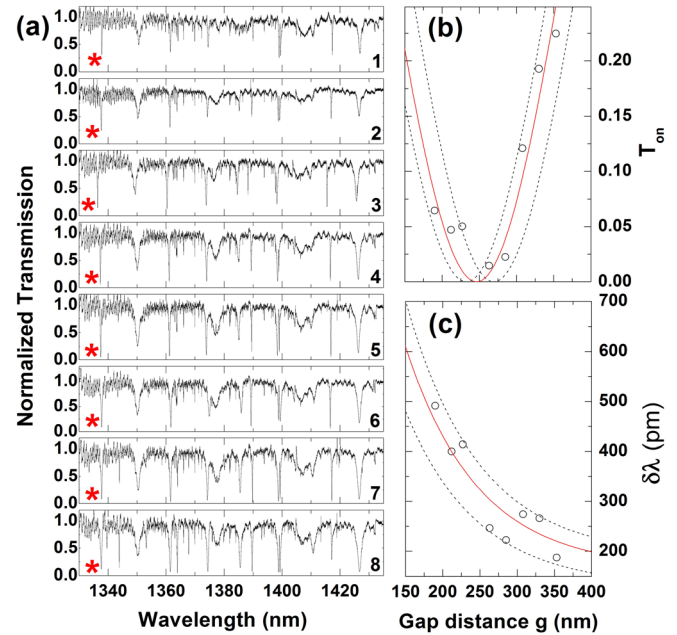


FIG. 3. (Color online) (a) Transmission spectra of suspended waveguides coupled to GaAs disks. From spectrum 1–8,  $g$  diminishes from 350 to 190 nm in steps of 25 nm. (b)  $T_{\text{on}}$  as a function of  $g$ , for the resonance marked with a star in (a). The open symbol size represents experimental uncertainties in  $g$  and  $T_{\text{on}}$ . (c) Width of the same resonance as a function of  $g$ .

Let us follow in detail the resonance marked with a star in Fig. 3(a). Figs. 3(b) and 3(c) show its on-resonance normalized transmission  $T_{\text{on}}$  and its linewidth  $\delta\lambda$  as a function of  $g$ . As  $g$  decreases, the overlap between the WGM and the guide mode increases, increasing evanescent coupling. In Fig. 3(b),  $T_{\text{on}}$  decreases when  $g$  decreases, before reaching zero at critical coupling for  $g = 250 \text{ nm}$ . Smaller  $g$ -values make the system enter the over-coupled regime, where coupling losses overcome intrinsic losses. In Fig. 3(c),  $\delta\lambda$  is enlarged as  $g$  decreases, reflecting again losses of the WGM due to its coupling to the guide.

CMT can describe the disk/guide evanescent coupling and its transition from the under to over-coupled regime. A heuristic CMT (Ref. 20) approach leads to simple expressions  $T_{\text{on}} = [(1 - \gamma_e/\gamma_i)/(1 + \gamma_e/\gamma_i)]^2$  and  $\delta\lambda = (\lambda_0/Q_{\text{int}})(1 + \gamma_e/\gamma_i)$ , where  $\gamma_e$  is the extrinsic WGM-to-guide coupling rate,  $\gamma_i = (2\pi c/\lambda_0)/Q_{\text{int}}$  is the intrinsic WGM loss rate,  $\lambda_0$  the WGM resonance wavelength, and  $Q_{\text{int}}$  the related intrinsic  $Q$ . These expressions were used to describe fiber taper evanescent coupling experiments with  $\gamma_e$  taken as a parameter varying exponentially with the gap distance  $g$ :<sup>8,24,25</sup>  $\gamma_e(g) = \gamma_e(0) \exp(-\eta g)$ , with  $\eta$  the inverse of the evanescent coupling decay length. In Fig. 3(b), the solid line is a fit using this exponential approximation and the above formula for  $T_{\text{on}}$ , taking  $\gamma_e(0)/\gamma_i$  and  $\eta$  as adjustable parameters. The best agreement is obtained for  $\gamma_e(0)/\gamma_i = 12.6$  and  $\eta = 1/97 \text{ nm}^{-1}$ . In Fig. 3(c), the solid line corresponds to the above formula for  $\delta\lambda$ , for the same fit parameters as above and where we use  $Q_{\text{int}} = 8100$ . However, nanofabrication tolerances result in slightly different disk and waveguide for each targeted gap distance. Amongst others,  $Q_{\text{int}}$  cannot be considered as a constant when we vary  $g$ . In Fig. 3(c), we capture this variability by bounding the results with two dashed

curves, obtained with the same value of  $\gamma_e(0)/\gamma_i$  and two bounding values of  $Q_{\text{int}} = 7040$  and  $10280$ . These bounding values are injected back in the formula for  $T_{\text{on}}$ , with the same value of  $\eta$  and with  $\gamma_e(0)$  extracted from  $\gamma_e(0)/\gamma_i = 12.6$  and from the average  $Q_{\text{int}}$  of  $8100$ . This leads to the two dashed curves of Fig. 3(b), which correctly bound the experimental results. To summarize, our experimental data are explained by a variability of  $\pm 20\%$  of  $Q_{\text{int}}$ . We note however that a full parameter-free modeling would necessitate to abandon the exponential approximation for  $\gamma_e$  and consider the exact evolution of  $\gamma_e(g)$  for each disk-waveguide couple.

Finally, in our disk/guide device, we can modify the evanescent tail of the waveguide mode by changing the width of the central taper, circumventing the difficulty of bringing the disk and guide arbitrarily close to one another. We used this approach by varying the taper width in steps of  $20\text{ nm}$ , from  $380$  to  $280\text{ nm}$ , for constant  $g = 220\text{ nm}$ , and could also obtain under-coupling, critical coupling, and over-coupling regimes.

In summary, we developed an integrated GaAs disk/waveguide system, where the nanoscale tapered part of the guide couples critically to WGMs. Our system offers integrated optical access to on-chip GaAs cavities of sub-micron mode volume and high  $Q$ . Perspectives include integrated quantum optomechanics experiments,<sup>26–29</sup> benefiting from the strong optomechanical coupling of GaAs disk resonators.<sup>6,7</sup> The GaAs platform would additionally allow for coupling active optical elements, possibly electrically pumped, to optomechanical functionalities.

This work was supported by C-Nano Ile de France and the French ANR.

<sup>1</sup>B. Gayral, J. M. Gerard, A. Lemaitre, C. Dupuis, L. Manin, and J. L. Pelouard, *Appl. Phys. Lett.* **75**, 1908 (1999).

<sup>2</sup>A. Kiraz, P. Michler, C. Becher, B. Gayral, A. Imamoglu, L. Zhang, E. Hu, W. V. Schoenfeld, and P. M. Petroff, *Appl. Phys. Lett.* **78**, 3932 (2001).

<sup>3</sup>E. Peter, P. Senellart, D. Martrou, A. Lemaître, J. Hours, J. M. Gérard, and J. Bloch, *Phys. Rev. Lett.* **95**, 067401 (2005).

- <sup>4</sup>S. L. McCall, A. F. J. Levi, R. E. Slusher, S. J. Pearton, and R. A. Logan, *Appl. Phys. Lett.* **60**, 289 (1992).
- <sup>5</sup>A. Andronico, I. Favero, and G. Leo, *Opt. Lett.* **33**, 2026 (2008).
- <sup>6</sup>L. Ding, C. Baker, P. Senellart, A. Lemaitre, S. Ducci, G. Leo, and I. Favero, *Phys. Rev. Lett.* **105**, 263903 (2010).
- <sup>7</sup>L. Ding, C. Baker, P. Senellart, A. Lemaitre, S. Ducci, G. Leo, and I. Favero, *Appl. Phys. Lett.* **98**, 113108 (2011).
- <sup>8</sup>L. Ding, P. Senellart, A. Lemaitre, S. Ducci, G. Leo, and I. Favero, *Proc. SPIE* **7712**, 771211 (2010).
- <sup>9</sup>C. P. Michael, K. Srinivasan, T. J. Johnson, O. Painter, K. H. Lee, K. Hennessee, H. Kim, and E. Hu, *Appl. Phys. Lett.* **90**, 051108 (2007).
- <sup>10</sup>L. Ding, C. Belacel, S. Ducci, G. Leo, and I. Favero, *Appl. Opt.* **49**, 2441 (2010).
- <sup>11</sup>D. Rafizadeh, J. P. Zhang, R. C. Tiberio, and S. T. Ho, *J. Lightwave Technol.* **16**, 1308 (1998).
- <sup>12</sup>S. Koseki, B. Zhang, K. De Greve, and Y. Yamamoto, *Appl. Phys. Lett.* **94**, 051110 (2009).
- <sup>13</sup>M. Cai, O. Painter, and K. J. Vahala, *Phys. Rev. Lett.* **85**, 74 (2000).
- <sup>14</sup>I. Favero and K. Karrai, *Nat. Photonics* **3**(4), 201 (2009).
- <sup>15</sup>F. Marquardt and S. Girvin, *Physics* **2**, 40 (2009).
- <sup>16</sup>M. Aspelmeyer, S. Gröblacher, K. Hammerer, and N. Kiesel, *J. Opt. Soc. Am. B* **27**, 189 (2010).
- <sup>17</sup>C. Hohberger and K. Karrai, in *Proceedings of 4th IEEE Conference on Nanotechnology* (IEEE, New York, 2004), pp. 419–421.
- <sup>18</sup>T. Carmon, H. Rokhsari, L. Yang, T. J. Kippenberg, and K. J. Vahala, *Phys. Rev. Lett.* **94**, 223902 (2005).
- <sup>19</sup>C. Metzger, M. Ludwig, C. Neuenhahn, A. Ortlieb, I. Favero, K. Karrai, and F. Marquardt, *Phys. Rev. Lett.* **101**, 133903 (2008).
- <sup>20</sup>C. Manolatou, M. J. Khan, S. Fan, P. R. Villeneuve, and H. A. Haus, *IEEE J. Quantum Electron.* **35**(9), 1322 (1999).
- <sup>21</sup>T. Kamalakis and T. Sphicopoulos, *IEEE J. Quantum Electron.* **42**(8), 827 (2006).
- <sup>22</sup>Y. F. Xiao, L. He, J. Zhu, and L. Yang, *Appl. Phys. Lett.* **94**, 231115 (2009).
- <sup>23</sup>A. Vörckel, M. Mönster, W. Henschel, P. H. Bolivar, and H. Kurz, *IEEE Photon. Technol. Lett.* **15**(7), 921 (2003).
- <sup>24</sup>M. Eichenfield, C. P. Michael, R. Perahia, and O. Painter, *Nat. Photonics* **1**, 416 (2007).
- <sup>25</sup>S. M. Spillane, T. J. Kippenberg, O. Painter, and K. J. Vahala, *Phys. Rev. Lett.* **91**(4), 043902 (2003).
- <sup>26</sup>M. Eichenfield, R. Camacho, J. Chan, K. J. Vahala, and O. Painter, *Nature* **459**, 550 (2009).
- <sup>27</sup>M. Li, W. H. P. Pernice, C. Xiong, T. Baehr-Jones, M. Hochberg, and H. X. Tang, *Nature* **456**, 480 (2008).
- <sup>28</sup>I. Favero, S. Stappner, D. Hunger, P. Paulitschke, J. Reichel, H. Lorenz, E. M. Weig, and K. Karrai, *Opt. Express* **15**, 12813 (2009).
- <sup>29</sup>D. Van Thourhout and J. Roels, *Nat. Photonics* **4**, 211 (2010).